ELSEVIER

Alzheimer's & Dementia 9 (2013) 499–511

Alzheimer's & Dementia

The synaptic proteome in Alzheimer's disease

Rachel Yoon Kyung Chang, Amanda S. Nouwens, Peter R. Dodd, Naomi Etheridge*

School of Chemistry and Molecular Biosciences, University of Queensland, Australia

Abstract

Background: Synaptic dysfunction occurs early in Alzheimer's disease (AD) and is recognized to be a primary pathological target for treatment. Synapse degeneration or dysfunction contributes to clinical signs of dementia through altered neuronal communication; the degree of synaptic loss correlates strongly with cognitive impairment. The molecular mechanisms underlying synaptic degeneration are still unclear, and identifying abnormally expressed synaptic proteins in AD brain will help to elucidate such mechanisms and to identify therapeutic targets that might slow AD progression.

Methods: Synaptosomal fractions from human autopsy brain tissue from subjects with AD (n = 6) and without AD (n = 6) were compared using two-dimensional differential in-gel electrophoresis. AD pathology is region specific; human subjects can be highly variable in age, medication, and other factors. To counter these factors, two vulnerable areas (the hippocampus and the temporal cortex) were compared with two relatively spared areas (the motor and occipital cortices) within each group. Proteins exhibiting significant changes in expression were identified ($\geq$20% change, Newman-Keuls P value $< .05$) using either matrix-assisted laser desorption ionization time-of-flight or electrospray ionisation quadrupole-time of flight mass spectrometry.

Results: Twenty-six different synaptic proteins exhibited more than twofold differences in expression between AD and normal subjects. These proteins are involved in regulating different cellular functions, including energy metabolism, signal transduction, vesicle transport, structure, and antioxidant activity.

Conclusion: Comparative proteome analysis uncovered markers of pathogenic mechanisms involved in synaptic dysfunction.

1. Introduction

Alzheimer's disease (AD) is an age-dependent neurodegenerative disorder that impairs cognitive and memory function progressively and is the most common form of dementia in the elderly [1]. Pathologically, AD is characterized by neuronal loss and the accumulation of neurofibrillary tangles and amyloid plaques. The magnitude of neuronal and synaptic loss correlate robustly with cognitive decline ante mortem [2]. Quantitative immunohistochemical and electron microscopic studies show significant, area-specific decreases in synaptic density in AD brain [2]. The hippocampus is the most severely affected region and the occipital cortex is the least [3]. Davis et al. [4] found a 25% to 35% decrease in the density of synapses and a 15% to 35% loss in the number of synapses per neuron in the frontal and temporal cortex.

The synapses that remain are functionally impaired in AD patients [5]. Even if they appear to be intact structurally, they may be dysfunctional. Defects in synthesis, transport, release, and reuptake of neurotransmitters; altered vesicle trafficking [6]; reduced metabolic activity; reduced or altered transmitter receptors, pumps, transporters, and ion channels; and defects in second messenger systems can alter synaptic function and impair synaptic maintenance, which can lead to excitotoxicity and, ultimately, memory impairment [7]. Synapses are a prime therapeutic target because synapse degeneration occurs early during the neurodegenerative processes.

During the past decade, various proteomic techniques have been used to study AD-induced changes in human brain. Sultana et al. [8] identified proteins expressed differentially in hippocampal cell lysates from AD autopsied brain. Proteins involved in energy metabolism, scaffolding,

*Corresponding author. Tel.: +61-7-3365-4614; Fax: +61-7-3365-4344.

E-mail address: n.etheridge@uq.edu.au

1552-5260/$ - see front matter © 2013 The Alzheimer's Association. All rights reserved.
http://dx.doi.org/10.1016/j.jalz.2012.04.009

pH regulation, cell cycle, tau phosphorylation, amyloid beta (Aβ) production, and antioxidant function were expressed differentially [8].

Two-dimensional differential in-gel electrophoresis (2D-DIGE) is an effective, widely used quantitative proteomics technique that labels protein extracts with three spectrally distinct fluorescent dyes, thus allowing different samples to be run on the same gel and to be visualized separately, and for expression differences between samples to be analyzed accurately. Enriched subcellular fractions increase the coverage of the proteome of a complex sample, including brain tissue [9], which enhances 2D-DIGE detection of low-abundance proteins and signaling complexes while reducing sample complexity [10]. A study of drug addiction used this technique to investigate the expression of synaptosomal proteins in the cortex, and found 27 proteins to be regulated differentially [11]. A study of AD-conditioned cultured cells used subcellular fractionation to identify oxidized synaptosomal proteins [12].

Despite the strong correlation between synaptic degeneration and cognitive decline in AD, synaptosomal fractions from human AD postmortem brain tissue have not been studied extensively. The aim of this study was to compare the expression of synaptosomal proteins in AD-affected and relatively spared areas in subjects with AD and non-AD normal subjects. We assessed the influences of possible confounds such as age, sex, and postmortem interval [13]. This is the first study that combined synaptosomal fractions with a top-down proteomics approach to examine the profile of synaptic proteins in autopsy brain tissue from AD patients. A recent study that used targeted Western blotting on fluorescence-activated cell sorter-sorted synaptosomes from autopsy tissue highlighted the colocalization of Na^+–Ca^{2+} exchangers with Aβ. It uncovered eight proteins not previously known to be associated with AD [14].

2. Methods

2.1. Tissue collection and storage

Brain tissue was obtained from the Queensland Brain Bank, School of Chemistry and Molecular Biosciences, University of Queensland, a node of the National Health and Medical Research Council–supported Australian Brain Bank Network, with informed written consent from the next of kin. Postmortem histopathological examination was conducted by qualified neuropathologists according to current Australian guidelines for the Consortium to Establish a Registry of Alzheimer's Disease criteria to confirm AD diagnosis [15]; none of the non-AD subjects met these criteria. Brain tissues collected at autopsy were immersed immediately in ice-cold isotonic sucrose solution (0.32 M) for cryoprotection and frozen slowly for storage at −80°C prior to further processing [16].

2.2. Case selection

Both pathologically affected and spared areas of the brain were selected to control for case-to-case variation, postmortem delay, and age-related factors [17]. Two severely affected areas, the hippocampus and the inferior temporal gyrus, together with the relatively spared occipital and motor cortices were obtained from each of six subjects without AD (age range, 69–87 years) and six women with AD (age range, 71–90 years). All subjects were white women of northern European ancestry. Postmortem intervals ranged from 8 to 49 hours; subject groups were closely matched first on this parameter, then on age (Supplementary Table 1). The literature suggests that most brain proteins are quite stable over such postmortem intervals [17,18], and that ethnicity does not influence AD progression significantly. The tissue retrieval method used has been optimized to maximize recovery of components [16]. As expected, the subjects with AD had a significantly smaller mean brain weight than normal subjects ($t_{10} = 3.057$, $P = .012$; Supplementary Table 1). The hippocampus and temporal lobe were chosen because these areas are severely damaged in AD. Motor and occipital cortices were selected as controls because they are both cortical regions, but are relatively less vulnerable to pathology in AD brain.

2.3. Sample preparation

Synaptosomes were prepared as described previously [19]. In brief, 0.5 g tissue from each of the four cortical areas was used. Rapidly thawed tissue was placed in a motor-driven Teflon-glass homogenizer with 10 volumes of ice-cold 0.32 M sucrose and homogenized, then centrifuged at 750*g* for 10 minutes at 4°C. The pellet was discarded and the supernatant centrifuged at 19,000*g* for 20 minutes at 4°C. The pellet was resuspended in 10 volumes of 0.32 M sucrose, layered onto a sucrose step gradient (0.8 M sucrose and 1.2 M sucrose), and centrifuged at 82,500*g* in a swinging bucket rotor (SW41Ti, Beckman L8-60M ultracentrifuge; Beckman Coulter, Brea, CA, USA) for 2 h at 4°C. The layer between 0.8 M and 1.2 M sucrose containing the synaptosomal fraction was collected.

2.3.1. Protein precipitation

Synaptosomal fractions were mixed with 1/9 volume of 0.4% deoxycholic acid and incubated on ice for 30 minutes. One molar trichloroacetic acid (1/9 volume) was added to the mixture and incubated on ice for 60 minutes. Samples were centrifuged at 10,000*g* for 10 minutes. Ice-cold 90% (v/v) acetone (1 mL) was added to the pellets and the resuspended samples were incubated at –20°C overnight. After centrifugation at 10,000*g* for 20 minutes, 1 mL ice-cold 90% acetone was added to the pellets and the samples were incubated at –20°C for 120 minutes. Samples were centrifuged at 10,000*g* for 20 minutes, and the pellets were dried for 5 minutes and resuspended in

CyDye (GE Healthcare Life Sciences, Piscataway, NJ, USA) labeling buffer (7 M urea, 2 M thiourea, 30 mM Tris, and 4% w/v 3-[(3-cholamidopropyl)dimethylammonio]-1-propanesulfonate [CHAPS]). The concentrations of synaptosomal proteins were assayed using the 2D-Quant kit (GE Healthcare Life Sciences) according to the manufacturer's instructions.

2.4. Two-dimensional differential in-gel electrophoresis

2.4.1. CyDye labeling

Aliquots of each synaptosomal sample were labeled with CyDye Fluors as described in the CyDye DIGE Fluors (minimal dye) Labeling Kit (GE Healthcare Life Sciences) with some modifications. Each sample (15 μg) was made up to a final volume of 9.5 μL with CyDye labeling buffer. A CyDye working solution consisting of 294 μM CyDye was made with fresh dimethylformamide, and 0.5 μL was added to each sample. After 30 minutes of incubation on ice in the dark, 1 μL of 10 mM lysine in water was added and the mixture was left on ice in the dark for 10 minutes. An internal standard was prepared by mixing 16.5 μg of each sample from all four brain areas and both groups (subjects with and without AD). The internal standard was divided into 24 × 15-μg aliquots and labeled with Cy2. The CyDye swap approach was used to minimize the variance in the efficiency of CyDye labeling. Half of each AD and non-AD sample from each brain region (hippocampus, temporal, occipital, and motor) was labeled with Cy5 and the other half with Cy3 so that dyes were swapped equally between the samples from the two groups.

2.4.2. Two-dimensional electrophoresis

One Cy2-labeled internal standard aliquot was mixed with one Cy5-labeled sample and the Cy3-labeled sample. One volume of sample buffer (8 M urea, 80 mM dithiothreitol, 4% CHAPS, 2% v/v immobilized pH gradient [IPG] buffer 3-11 nonlinear [NL; GE Healthcare Life Sciences]) was added to the labeled sample and incubated on ice for 10 minutes in the dark. Sample volume was brought up to 450 μL with rehydration buffer (8 M urea, 13 mM dithiothreitol, 4% w/v CHAPS, 1% v/v IPG buffer 3-11 NL) and was mixed thoroughly. Samples were loaded onto 24-cm Immobiline DryStrip pH 3-11 NL IPG strips (GE Healthcare Life Sciences) and isoelectric focusing was conducted using an Ettan IPGphor II isoelectric focusing system (GE Healthcare Life Sciences) with a 12-hour active rehydration step followed by 500 V for 2 hours, 1000 V for 1 hour, then 8000 V until 40,000 total V-hours was reached. After focusing, IPG strips were equilibrated in buffer (50 mM Tris-Cl pH 8.8, 6 M urea, 2% [w/v] sodium dodecyl sulfate, 30% [v/v], glycerol 0.002% [w/v] bromophenol blue) containing 0.1% (w/v) dithiothreitol for 15 minutes, then the dithiothreitol in the buffer was replaced by 0.25% (w/v) idoacetamide for 15 minutes. Equilibrated IPG strips were loaded onto 24-cm 10% acrylamide sodium dodecyl sulfate-polyacrylamide gel electrophoresis gels and embedded in 0.5% (w/v) agarose in running buffer (25 mM Tris, 250 mM glycine, 0.1% [w/v] sodium dodecyl sulfate) with 0.002% (w/v) bromophenol blue. Second-dimension separation was performed on an Ettan DALT 12 separation unit (GE Healthcare Life Sciences) running at 2 W/gel for 30 minutes, 5 W/gel for 30 minutes, 10 W/gel for 2.5 hours, then 15 W/gel until the bromophenol blue dye front was approximately 1 mm from the bottom of the gel.

2.5. Comparative image analysis

Gels were scanned on a Typhoon 9400 scanner (GE Healthcare Life Sciences) at three wavelengths (Cy2, 488 nm; Cy3, 532 nm; Cy5, 633 nm) and the fluorescence intensity at 520 nm (Cy2), 580 nm (Cy3), and 670 nm (Cy5) was measured. ImageQuant (GE Healthcare Life Sciences) was used to crop and rotate the images, and all gel images were aligned using the TT900 S2S (Nonlinear Dynamics, Newcastle upon Tyne, UK) alignment module. After alignment, each spot from every sample was scrutinized to ensure that the software had selected and outlined a discrete protein spot. Magnified 2D and three-dimensional montage views allowed incompletely separated spots to be separated manually. Unresolved smears were removed from the analysis. Aligned gels were analyzed automatically using the Progenesis PG240 SameSpots module (Nonlinear Dynamics) with background subtraction and radiometric normalization. Normalized volumes of protein spots were compared to determine expression differences between groups and regions. Normalized volumes of each spot from all 24 gels were analyzed using Statistica (Statsoft, Tulsa, OK, USA). Proteins exhibiting significant changes (Newman-Keuls P value $<$ .05; fold change, $>$20%) were analyzed in this study.

2.6. Protein identification

2.6.1. Trypsin digest

For protein excision and identification, additional two-dimensional electrophoresis gels were run with increased amounts of protein. Pooled protein samples (700 μg from subjects with and without AD without the internal standard) were separated using the same conditions as described but without CyDye labeling. After the second dimension, gels were fixed in 50% v/v ethanol/2% v/v o-phosphoric acid overnight, washed in water, then stained in 34% v/v methanol, 17% w/v ammonium sulfate, 3% v/v o-phosphoric acid, and 0.066% w/v colloidal Coomassie Brilliant Blue G250 (Fluka, Buchs, Switzerland) for 2 days. Protein spots considered statistically significant in comparative image analysis were excised and stored in 1% acetic acid until further use. Excised gel plugs were washed in 25 mM ammonium bicarbonate/5% acetonitrile, then twice in 25 mM ammonium bicarbonate/50% acetonitrile (high-performance liquid

chromatography grade; Sigma, St. Louis, MO, USA) for 15 minutes each. Plugs were dried in an SPD Speedvac (Thermo Fisher Scientific, Waltham, MA, USA) at room temperature, followed by rehydration with 6 μL of 40 ng/μL trypsin in 25 mM ammonium bicarbonate at 4°C for 1 hour. An additional 25 mM of ammonium bicarbonate was added to prevent plug dehydration during incubation at 37°C overnight. Peptides were extracted from the samples with 15 μL of 0.1% (v/v) trifluoroacetic acid, then with 30 μL of 5% trifluoroacetic acid/50% (v/v) acetonitrile (twice) and concentrated in a Speedvac. Extracted peptide samples were analyzed either on a Voyager DE STR matrix-assisted laser desorption/ionisation time-of-flight (MALDI-TOF) or QSTAR Pulsar i electrospray ionisation (ESI)-quadrupole time-of-flight (QTOF) mass spectrometer (Applied Biosystems, Vernon Hills, IL, USA).

2.6.2. Matrix-assisted laser desorption ionization time-of-flight mass spectrometry

Dried peptides were resuspended in 1.5 μL matrix solution (5 μg/μL α-cyano-4-hydroxycinnamic acid, 60% acetonitrile, 0.1% [v/v] trifluoroacetic acid) then spotted onto a stainless steel sample plate. External calibrations of spectra were performed using a 0.5-μL calibration standard mixture (5 fmol/μL angiotensin I [Sigma], 5 fmol/μL adrenocorticotropic hormone [1–17; Sigma], 3.75 fmol/μL adrenocorticotropic hormone [18–39; Sigma], 60% [v/v] acetonitrile, and 0.1% [v/v] trifluoroacetic acid). Spectra were acquired between 1000 m/z (mass-to-charge ratio) and 5000 m/z using a 25,000-V accelerating voltage and 68% grid voltage in reflectron mode. Delay time and laser intensity were optimized for each peptide mix. The spectra obtained were processed with baseline correction and smooth spectrum peak labeling, and were calibrated externally with calibration standards using Mmass [20].

2.6.3. Quadrupole time-of-flight mass spectrometry

Dried peptides were resuspended in 5% acetonitrile/0.1% trifluoroacetic acid and injected onto an 1100/1200 capLC system (Agilent Technologies, Santa Clara, CA, USA). Samples were first desalted on a C18 trap before valve switching and separation on an Agilent Zorbax SB300 C18 column (150 × 0.5 mm, 5 μm). The gradient was 0% to 60% buffer B from 0 to 60 minutes, 60% to 90% buffer B from 60 to 62 minutes, 90% buffer B from 62 to 65 minutes, and 90% to 0% buffer B from 65 to 67 minutes, where buffer A contained 5% acetonitrile/0.1% formic acid and buffer B contained 0.1% trifluoroacetic acid in acetonitrile. Eluted peptides were passed directly to a QSTAR Pulsar in positive-ion mode equipped with a standard ion spray source. Spectra were acquired over the 350 to 1,600 m/z range for 1 second, followed by data-dependent mass spectrometry (MS)/MS fragmentation of the top three most intense ions for 2 seconds, followed by dynamic exclusion for 180 seconds. Files were converted to Mascot [21] generic format for database searching.

2.6.4. Database searching

Protein identities were determined by searching the SwissProt database using Mascot (Matrix Science, London, UK; [21]) using the labeled peak masses in the resultant peptide mass fingerprint (PMF). Peptide tolerance was set to 300 ppm (0.03% difference). For all database searches, carbamidomethyl was set as a fixed modification, and methionine oxidation was variable. Similar settings were used for quadrupole time-of-flight (QTOF) data with the exception that error tolerance was set to 0.5 Da for MS and 0.2 Da for MS/MS. A protein match was considered accurate only with a significant Mascot probability score (>63 for MALDI-TOF, >39 during QTOF; *Homo sapiens* SwissProt database, $P < .05$) and, for PMF data, more than 15% sequence coverage.

3. Results

In total, 24 gels were run and 72 gel images were generated by visualization at each Cy-dye wavelength. These images, when analyzed with Progenesis SameSpots, detected a total of 871 protein spots across all 24 gels (Supplementary Fig. 1). Normalized volumes for each protein spot were analyzed using analysis of covariance, which revealed that neither age ($P = .58$) nor postmortem interval ($P = .55$), nor age and postmortem interval combined ($P = .56$), altered the data significantly (Fig. 1; Supplementary Fig. 2). A significant Newman-Keuls post hoc test ($P < .05$) plus a disparity greater than 20% between test sample and control were the criteria used to delineate a significant difference in protein expression.

3.1. Spared areas in subjects with and without AD

2D gels representing areas that are relatively spared in the AD brain were compared in AD and non-AD samples (AD motor vs. non-AD motor, and AD occipital vs. non-AD occipital cortices). In the motor cortex comparison, no significant difference in expression was observed for any protein spot. In the occipital cortex, the expression of one protein differed significantly between subjects with and without AD (140%; $P = .013$). This spot was of low abundance. It cannot be detected visually with colloidal Coomassie staining and was only stained faintly by silver; it could not be identified by MS. These comparisons demonstrate that the relatively spared areas of AD brain—motor and occipital cortices—can be used as control regions to normalize expression in more affected areas.

3.1.1. Hippocampus versus spared areas

A total of 78 synaptic proteins showed significant differences in relative expression in AD hippocampus compared with AD occipital cortex, whereas 60 proteins differed in non-AD hippocampus from non-AD occipital cortex. Of the proteins that differed, 33 were in common in the AD/non-AD comparisons (Fig. 1A). When the motor cortex

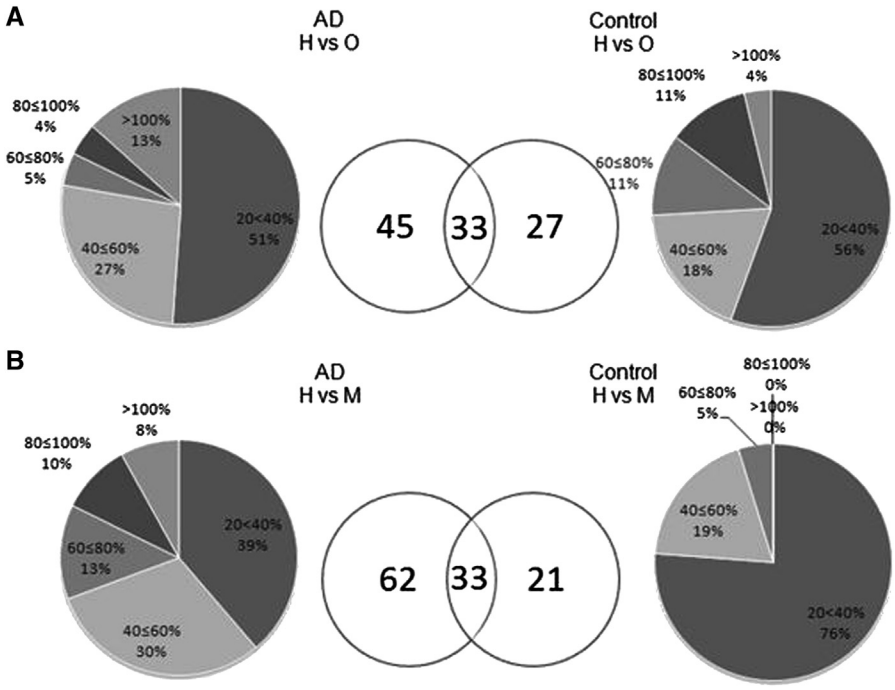

Fig. 1. Numbers of proteins exhibiting significantly altered expression between (A) hippocampus (H) and occipital cortex (O), and (B) hippocampus and motor cortex (M) in subjects with (AD) and without (Control) Alzheimer's disease. Pie charts show numbers of proteins at each level of percentage change. Venn diagrams indicate numbers of unique and in-common proteins within each comparison.

was used as the control, the levels of 62 protein spots differed significantly in AD hippocampus (21 spots in non-AD hippocampus) with 33 spots in common (Fig. 1B). Of the shared protein spots in the hippocampus versus the occipital lobe and the hippocampus versus the motor cortex comparisons, 55% were found to have the same spot numbers (Table 1).

3.1.2. Temporal cortex versus spared areas

The number of proteins expressed differentially was lower in the temporal cortex than in the hippocampus. The comparison between the temporal and occipital cortices detected a total of 22 protein spots expressed differentially in subjects with AD, and 44 protein spots in subjects without AD, and there were four spots in common (Fig. 2A). Comparison between the temporal and motor cortices detected four differentially regulated protein spots in AD and 31 in non-AD, with one spot in common (Fig. 2B). Surprisingly, the number of proteins and the extent of expression difference were relatively stronger in non-AD brain, with a greater number of proteins showing lower percentage differences in AD.

3.1.3. Hippocampus versus temporal cortex

The degree of synaptic degeneration is high in AD hippocampus, with synaptic loss up to 55% compared with temporal cortex at 15% to 35%. The two affected regions were compared to determine whether such differences might affect the number of proteins that showed significantly altered expression. With the occipital cortex as control, 45 synaptic proteins showed expression differences in AD hippocampus, and 18 proteins in temporal cortex. With the motor cortex as control, 62 proteins in AD hippocampus and 3 proteins in AD temporal cortex showed significant differences in expression. Of the proteins that showed altered expression in AD hippocampus, 27 were detected both in the occipital cortex and motor cortex comparisons; of the proteins exhibiting expression differences in AD temporal cortex, two were detected in both comparisons.

3.2. Protein identification

Protein spots exhibiting significant expression differences (>20%) between affected and spared regions were identified by either MALDI-ToF or electrospray ionization time-of-flight MS analysis. To obtain sufficient material for MALDI-ToF MS, preparative 2D gels were loaded with 700 μg protein and visualized with colloidal Coomassie staining. Protein spots excised from the gels were "trypsinized" and subjected to PMF analysis (Table 1). Quadrupole time of flight was used to identify faint spots containing less-abundant peptides (Table 2).

A total of 52 spots were identified; a few spots of interest could not be identified because the sensitivity of Coomassie staining is less than that of fluorescent labeling. The proteins identified are associated with energy metabolism, vesicular transport, structure, protein chaperones, and neurotransmitter synthesis. Several proteins regulated differentially in AD-affected areas were identified at multiple positions on the 2D gel. These may represent different isoforms or posttranslationally modified forms of the same protein (Fig. 3).

Table 1
Proteins identified using matrix-assisted laser desorption ionization time-of-flight mass spectrometry that are expressed differentially in Alzheimer's disease (AD)-affected regions compared with relatively spared regions

Spot no.	SwissProt accession no.	Mascot score	Cover, %	Mr, kDa	pI	Identification	AD		Non-AD	
							Change, %	*P* value	Change, %	*P* value
Hippocampus vs. motor cortex										
25	P18669	80	38	29	6.67	Phosphoglycerate mutase 1	60.5	*.004*	25.8	.566
32	P31150	68	26	23	5.02	Rab GDP-dissociation inhibitor α	38.8	*.028*	34.8	.058
67	P12277	123	37	43	5.34	Creatine kinase B-type	−21.2	*.001*	−14.6	.062
119	Q9NZN3	95	19	61	6.12	EH domain-containing protein 3	−28.2	*.039*	−22.6	.147
522	Q16555	92	22	63	5.95	Dihydropyrimidinase-related protein 2	52.5	*.001*	37.9	.205
550	Q92599	67	22	50	5.77	Septin-8	24.9	*.0005*	7.2	*.018*
565	P00367	94	23	62	7.66	Glutamate dehydrogenase 1	29.5	*.017*	38.7	.904
590	P06733	110	39	47	6.99	α-Enolase	53.1	*.004*	41.9	.642
642	P15104	97	22	43	6.43	Glutamine synthetase	−50.7	*.017*	−51.8	.075
671	P60709	106	28	42	5.29	β-Actin	98.9	*.0003*	75.9	.757
711	P40925	76	26	32	7.62	Malate dehydrogenase	56.5	*.003*	13.8	.789
726	Q71U36	73	24	51	5.02	α-Tubulin	40.2	*.035*	25.0	.180
794	Q96E11	74	26	29	9.80	Ribosome recycling factor	56.8	*.030*	18.5	*.024*
839	A6NLJ7	106	46	25	5.33	Ubiquitin thiolesterase	37.3	*.047*	34.4	.986
866	Q06830	74	39	22	8.27	Peroxiredoxin 1	71.4	*.001*	10.6	.090
30	P52565	70	29	23	5.02	ρ GDP dissociation inhibitor 1	26.2	.084	33.6	*.033*
232.1	Q9Y2T3	76	26	45	5.19	Guanine deaminase	49.5	.148	83.5	*.049*
566	Q92599	78	22	56	5.89	Septin-8	16.6	.161	−21.4	*.015*
612	P09104	77	26	48	4.91	Enolase, γ	−18.1	.058	−25.2	*.010*
645	P15104	124	22	43	6.43	Glutamine synthetase	−35.2	.122	−38.6	*.002*
Hippocampus vs. occipital Cortex										
25	P18669	80	38	29	6.67	Phosphoglycerate mutase 1	44.3	*.014*	10.3	.757
67	P12277	123	37	43	5.34	Creatine kinase B-type	−23.9	*.001*	−6.0	.427
81	P17174	129	37	40	6.41	Aspartate aminotransferase	−29.1	*.023*	−10.0	.594
131	P14618	107	24	59	7.6	Pyruvate kinase	−32.4	*.002*	−7.7	.865
308.1	P60709	66	27	42	5.29	α-Actin	24.5	*.023*	16.1	.217
612	P09104	77	26	48	4.91	γ-Enolase	−27.4	*.009*	−12.4	.470
711	P40925	76	26	32	7.62	Malate dehydrogenase	59.3	*.003*	17.9	.399
726	Q71U36	73	24	51	5.02	α-Tubulin	53.7	*.005*	23.8	.153
866	Q06830	74	39	22	8.27	Peroxiredoxin 1	47.8	*.004*	7.1	.884
30	P52565	70	29	12	5.02	ρ GDP dissociation inhibitor 1	17.0	.375	34.4	*.012*
105	P11142	69	21	71	5.37	Heat shock cognate 71 kDa protein	13.6	.515	33.9	*.035*
106	P11142	72	24	71	5.37	Heat shock cognate 71 kDa protein	17.3	.156	21.2	*.050*
351	Q8WUM4	90	21	97	6.13	Programmed cell death 6 interacting protein	22.4	.229	33.1	*.016*
485	Q14194	82	21	62	6.55	Dihydropyrimidinase-related protein 1	0.3	.975	25.1	*.047*
652	P09972	82	28	40	6.41	Fructose-bisphosphate aldolase C	39.0	.407	72.8	*.039*
Temporal cortex vs. occipital cortex										
32	P31150	68	26	23	5.02	Rab GDP dissociation inhibitor α	40.1	*.031*	1.6	.896
543	O43175	68	23	57	6.29	D-3-phosphoglycerate dehydrogenase	41.1	*.049*	28.1	.286
30	P52565	70	29	23	5.02	ρ GDP dissociation inhibitor 1	22.9	.127	32.8	*.008*
521	Q9BZV1	73	29	50	6.46	UBX domain-containing protein 6	8.2	.274	22.4	*.0004*
538	P55809	86	30	57	7.14	Succinyl-coenzyme A:3-ketoacid-coenzyme A transferase 1	4.8	.592	46.9	*.001*
566	Q92599	78	22	56	5.89	Septin-8	1.5	.865	−21.0	*.025*
568	Q9NVA2	69	25	50	6.36	Septin-11	7.8	.665	34.4	*.0001*
686	P09471	72	21	41	5.34	G(o) protein, subunit α	−4.4	.222	−20.6	*.043*
690	P09471	70	22	41	5.34	G(o) protein, subunit α	−4.2	.695	−38.6	*.015*
Temporal cortex vs. motor cortex										
131	P14618	107	24	59	7.60	Pyruvate kinase	−22.5	*.032*	−2.2	.988
543	O43175	68	23	57	6.29	D-3-phosphoglycerate dehydrogenase	49.0	*.031*	28.1	.209
690	P09471	70	22	41	5.34	G(o) protein, subunit α	35.9	*.027*	−14.7	.368
30	P52565	70	29	23	5.02	ρ GDP dissociation inhibitor 1	13.7	.462	33.5	*.011*
105	P11142	69	21	71	5.37	Heat shock cognate 71-kDa protein	10.0	.567	30.7	*.044*
106	P11142	72	24	71	5.37	Heat shock cognate 71-kDa protein	8.4	.448	24.8	*.025*
232.1	Q9Y2T3	76	26	45	5.19	Guanine deaminase	49.0	.155	61.3	*.047*

(*Continued*)

Table 1
Proteins identified using matrix-assisted laser desorption ionization time-of-flight mass spectrometry that are expressed differentially in Alzheimer's disease (AD)-affected regions compared with relatively spared regions (*Continued*)

Spot no.	SwissProt accession no.	Mascot score	Cover, %	Mr, kDa	pI	Identification	AD		Non-AD	
							Change, %	*P* value	Change, %	*P* value
521	Q9BZV1	73	29	50	6.46	UBX domain-containing protein 6	8.7	.312	24.0	*.0004*
819	O94811	107	39	24	9.48	Tubulin polymerization-promoting protein	1.8	.878	28.0	*.021*

Abbreviations: GDP, guanosine diphosphate; EH, Eps15 homology; UBX, ubiquitin regulatory X.

NOTE. Each protein is listed with Mascot score (SwissProt; significant if value is greater than 66), sequence coverage, theoretical molecular mass, isoelectric point, percent change (significant if value is greater than ~20%), and *P* value (generated by Newman-Keuls post hoc test; significant are in italics).

Twenty-six proteins showed more than twofold differences in expression in subjects with and without AD. Of these, 10 associated with vesicular trafficking (septin-11, septin-8, v-type proton adenosine triphosphatase (ATPase) catalytic subunit A, tubulin polymerization-promoting protein, ρ guanosine diphosphate (GDP)-dissociation inhibitor, heat shock cognate 71 kDa protein, dihydropyrimidase-related protein 1, α-tubulin, β-actin, and annexin A5) were chosen for pathway analysis using Ingenuity's IPA core analysis, which revealed that these proteins are associated closely with each other (Fig. 4).

4. Discussion

In this study, we used an enrichment procedure coupled with proteomics and MS to identify synaptosomal proteins that differ in expression between subjects with and without AD in two regions of brain that are severely affected in AD and two that are relatively spared. The protein changes were normalized by loading the same amount of synaptic proteins onto each gel. Previous quantitative studies examined protein expression in the total proteome of human AD hippocampus [8], a transgenic mouse model [22,23], and a selection of synaptic proteins in the frontal cortex of human autopsied AD brain [24]. To the best of our knowledge, this is the first study to look at the whole synaptosomal fraction from AD-affected areas of human brain using a top-down proteomics approach. We confirm, using our comparative technique, that pathologically spared areas in AD brain can indeed serve as a control for affected regions [17]. We identified 26 synaptic proteins that showed a mean expression difference of greater than 20% between affected and relatively spared areas in the same subject. The data set was examined with the Progenesis program, which has strong accuracy reproducibility, and only statistically significant expression differences were analyzed (see Methods). Hence, no further validation of the data was deemed necessary.

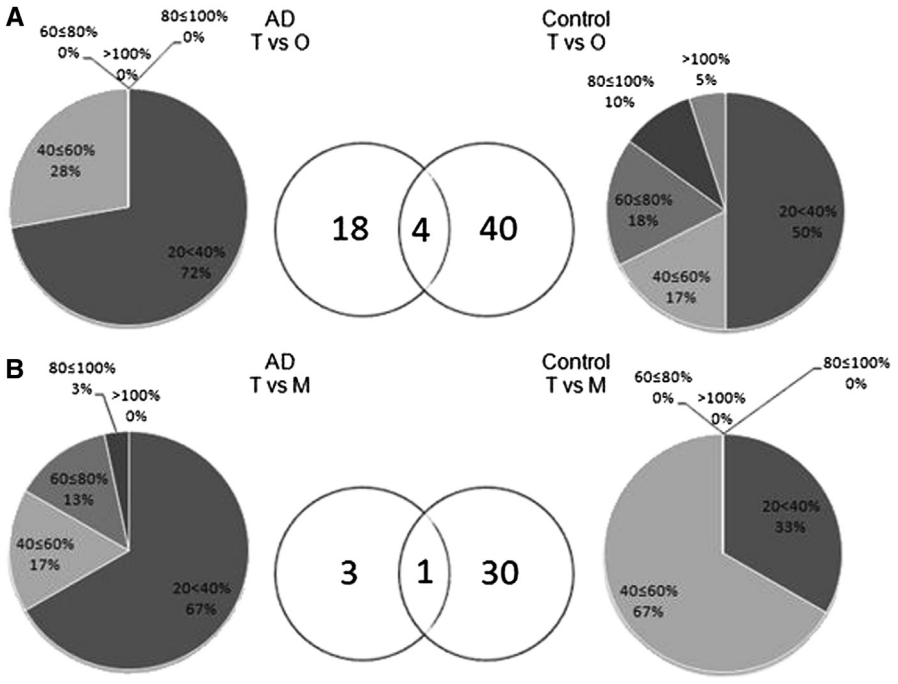

Fig. 2. Numbers of proteins exhibiting significantly altered expression between (A) the temporal (T) and occipital (O) cortices, (B) and the temporal and motor (M) cortices in subjects with (AD) and without Alzheimer's disease.

Table 2
Proteins identified using QTOF mass spectrometry that are expressed differentially in Alzheimer's disease (AD)-affected regions compared with relatively spared regions.

Spot no.	SwissProt accession no	Mascot score	Cover, %	Mr, kDa	pI	Identification	AD		Non-AD	
							Change, %	*P* value	Change, %	*P* value
Hippocampus vs. motor cortex										
277	P50395	149	8	51088	5.94	Rab GDP dissociation inhibitor β	39.3	*.005*	27.9	.081
673	P60709	217	12	42052	5.29	β-actin	193.0	*.0003*	80.8	.315
714	P21579	113	13	47885	8.26	Synaptotagmin-1	45.7	*.015*	44.1	.070
766	P08758	172	27	35971	4.94	Annexin A5	79.3	*.0001*	12.5	.486
825	P60709	352	20	42052	5.29	Actin	104.6	*.0008*	66.1	.062
696	Q8IXJ6	79	5	43782	5.22	NAD-dependent deacetylase sirtuin-2	−29.2	.172	−50.7	*.049*
Hippocampus vs. occipital cortex										
277	P50395	149	8	51088	5.94	Rab GDP dissociation inhibitor β	36.5	*.008*	12.2	.351
673	P60709	217	12	42052	5.29	β-Actin	198.8	*.0003*	80.0	.292
700	P06733	98	7	47481	7.01	α-Enolase	26.8	*.043*	16.1	.054
766	P08758	172	27	35971	4.94	Annexin A5	76.1	*.0001*	20.2	.631
824	P04792	233	26	22427	7.83	Heat shock protein 27	62.2	*.004*	50.4	.660
825	P60709	352	20	42052	5.29	Actin	86.6	*.002*	65.2	.187
845	P28161	79	16	25899	6	Glutathione S-transferase μ2	46.1	*.016*	12.0	.523
855	P30048	170	25	28017	7.67	Thioredoxin-dependent peroxide reductase	59.2	.054	40.6	*.036*
Temporal cortex vs. motor cortex										
700	P06733	98	7	47481	7.01	α-Enolase	−4.5	.617	−25.0	*.010*
Temporal cortex vs. occipital cortex										
107	P38606	67	19	68660	5.35	V-type proton ATPase catalytic subunit A	8.2	.709	39.4	*.012*
108	P38606	76	19	68660	5.35	V-type proton ATPase catalytic subunit A	−0.2	.984	30.0	*.020*
485	Q14194	82	21	62487	6.55	Dihydropyrimidinase-related protein 1	16.6	.314	33.9	*.006*

Abbreviations: ATPase, adenosine triphosphatase; GDP, guanosine diphosphate.

NOTE. Each protein is listed with Mascot score (SwissProt; significant if value is greater than 39), sequence coverage, theoretical molecular mass, isoelectric point, percentage change (significant if value is greater than ∼20%), and *P* value (generated by Newman-Keuls post hoc test; significant values are in italics).

Identification by MALDI-ToF or QTOF MS showed proteins involved in energy metabolism, vesicle trafficking, chaperoning, structural integrity, and signal transduction. During sample preparation, each protein spot was cut from the gel and washed with ethanol and water to avoid contamination. Proteins were identified by MS in combination with stringent Mascot search terms. Only intense peaks with low baselines were chosen a for MALDI-ToF-driven Mascot search, and the taxonomy was confined to *Homo sapiens* with a peptide tolerance of ±300 ppm (0.03% difference). For QTOF, the data error tolerance was set to 0.5 Da for MS and 0.2 Da for MS/MS. To avoid false identification through MALDI-ToF MS, only proteins with a percentage sequence of 19% or greater and a Mascot score of more than 66 (35 Mascot score for QTOF MS) were regarded as registering true identity. In current practice, MS does not need further validation as a result of the highly specific nature of MS and Mascot.

The number of synaptic proteins showing altered expression was greater in AD hippocampus than in AD temporal cortex, which is in accordance with the previous findings that the degree of synaptic loss is greater in hippocampus than in temporal cortex. Note, however, that the differences we observed did not derive from the loss of nerve endings, because equal amounts of protein from each sample region were loaded onto each gel. Thus, the number of proteins exhibiting expression differences may relate to the degree of pathology in AD, and represent altered protein expression within the remaining nerve endings. These differences could portray mechanisms underlying the loss of synaptic connections in human AD brain.

4.1. Vesicle-trafficking proteins

In addition to synaptic loss, synaptic function within an intact neuron is also affected in AD, as shown by previous studies in which synaptic vesicle trafficking was disrupted in AD [25]. Our results support this, with vesicle-related proteins—v-type proton ATPase catalytic V1 subunit A, annexin V and septin-8—found to exhibit significant expression changes in AD-affected areas. V-ATPases are synaptic vesicle membrane proteins that contain catalytic V1 and V0 domains [26]. The V1 domain helps the vesicle to accumulate neurotransmitters by reducing the intracellular pH by proton translocation across the membrane [27]. V-ATPase catalytic V1 subunit A was identified from two trains of spots (Fig. 3A), representing either isoforms or a result of post-translational modification, which showed lower expression

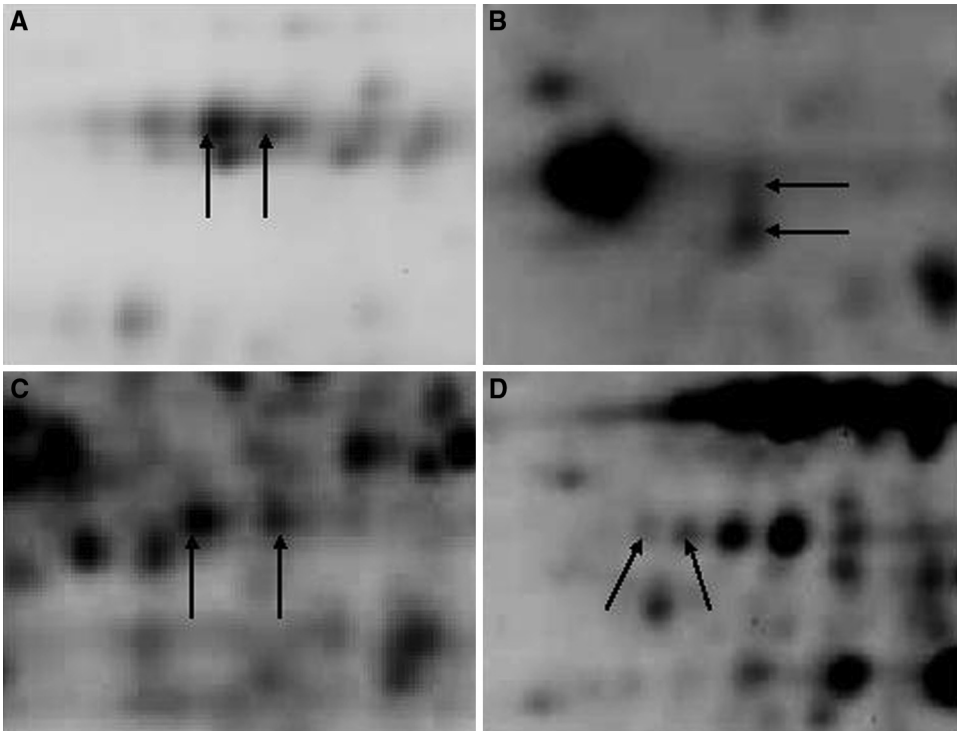

Fig. 3. Examples of proteins detected in trains of spots on the two-dimensional gel. (A) V-type proton adenosine triphosphatase catalytic subunit A. (B) ρ Guanine nucleotide dissociation inhibitor 1. (C) Septin 8. (D) G(o) Protein subunit α. In each instance, the spots indicated with arrowheads are comprised of the same protein.

in AD temporal cortex compared with non-AD temporal cortex (29% and 24%, respectively). This reduction may affect vesicular neurotransmitter accumulation and release, thereby altering neuronal communication.

In AD hippocampus, the expression of synaptic annexin V was greater by 76.1% (vs. motor cortex) and 79.3% (vs. occipital cortex). Annexin V associates with synaptic vesicles in the presence of high synaptoplasmic Ca^{2+} concentrations [28]. Although the functional role in vesicle trafficking is still to be determined, an increase in annexin V and calcium levels in AD brain may affect vesicle transport, and may alter protein recycling and neurotransmitter releases. Furthermore, the hydrophobic nature of annexin V may allow its interaction with membranes, where it can function as an ion channel and induce local disorder in the lipid bilayer [29], which may promote synaptic atrophy. On the positive side, annexin V protects against the cytotoxicity of Aβ in cell culture [30], which may explain its higher concentration in Aβ-rich areas. The occurrence of Aβ in AD synapses may promote increased annexin V expression, which has a deleterious effect on vesicle trafficking, ultimately damaging the neuron.

Septin-8 is enriched in synaptic vesicles, synaptic plasma membranes, and synaptosomal membranes [31]. In a CV-1 in origin carrying SV40 (COS)-7 cell expression system, immunoprecipitation assays revealed that septin-8 binds with vesicle associated membrane protein 2 (VAMP2) and that this interaction is reduced by Synaptosomal-Associated protein 25 kDa (SNAP25) [31]. Increased expression of septin-8 suppresses the binding of synaptophysin to VAMP2 [31], which suggests that septin-8 may regulate the soluble N-ethylmaleimide sensitive factor attachment protein receptor (SNARE) complex formation and subsequent exocytosis. The observed change in the expression of these synaptic vesicle-related proteins in AD synapses may affect neurotransmitter release and neuronal communication, thus affecting memory.

4.2. Structural proteins

The expression of structural proteins, including tubulin polymerization-promoting protein (TPPP), septin-11, dihydropyrimidinase-relate protein 1, and β-actin, differed in AD-affected areas. Disturbed expression of structural proteins could lead to a loss of structural integrity and cause synaptic atrophy. Synaptic cytoskeletal integrity is important in neuronal connections and communication, and is maintained by the regulation of structural proteins including tubulin. Tubulin, a major component of microtubules, controls membrane-bound organelle transportation to replenish supplies required for axonal growth and repair. Microtubule destabilization and related transport system failure is prevalent in AD [32], and may, in turn, be prevented by promoting microtubule integrity [33]. TPPP plays this preventive role in stabilizing microtubule structure, and may polymerize tubulin into microtubules.

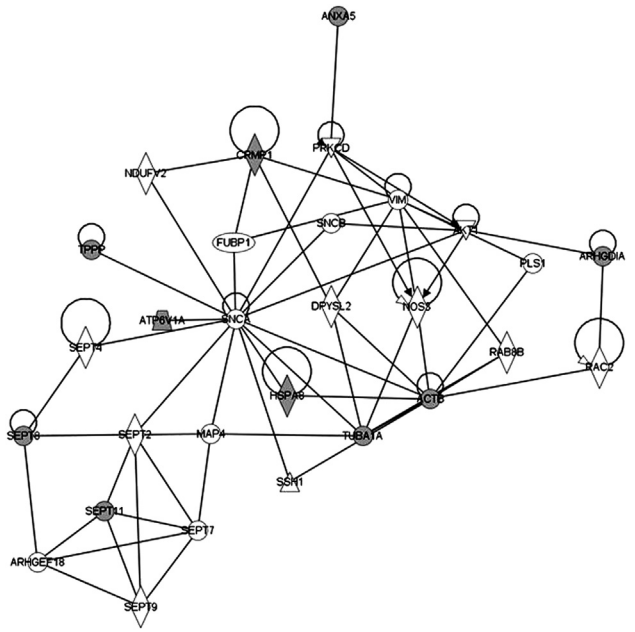

Fig. 4. Pathway analysis. Each symbol represents a class of protein (△ phosphatase, ▽ kinase, ◇ other enzyme, ○ other). Identified proteins are shaded. The interaction schema was generated using Ingenuity Pathway Analysis (Ingenuity Systems). ACTB, β-actin; ARHGDIA, r GDP-dissociation inhibitor; ATP6V1A, v-type proton ATPase catalytic subunit A; AXNA5, annexin A5; CRMP1, dihydropyrimidase-related protein 1; HSP A8, heat shock cognate 71 kDa protein; SEPT8, septin-8; SEPT11, septin-11; TPPP, tubulin polymerization-promoting protein; TUBA1A, tubulin α-1A chain.

Lowered expression of TPPP (24%) and septin-11 in AD temporal cortex (26%), compared with non-AD temporal cortex, may mediate the severe axon atrophy and synapse loss in AD-affected areas. Septin-11 also regulates synaptic structure maintenance; reduced dendritic arborization depletes this protein from cultured hippocampal neurons. Septin-11 may play a role in γ-aminobutyric acid-ergic synaptic connectivity [34]. β-Actin is part of the cytoskeletal complex and is popular as a loading control for AD studies [33]. It is interesting to note that its expression was twofold higher in the synaptic fraction of AD hippocampus than in non-AD hippocampus. This may reflect a compensatory response to strengthen or repair the remaining intact synapses and neurons. The function of structural protein dihydropyrimidinase-related protein 1 has not been characterized fully; however, a recent behavioral study suggested its possible role in spatial learning and hippocampal plasticity [35]. Hence, lower expression of dihydropyrimidinase-related protein 1 in AD hippocampus is consistent with the cognitive decline observed AD. The expression was greater by 25.1% in non-AD hippocampus, and no expression difference was found in AD hippocampus (data not significant). Altered expression of these structural proteins may be related to an impaired axonal transport mechanism and synaptic degeneration in pathologically affected areas of the AD brain.

4.3. Energy-related proteins

The brain is highly active metabolically, using up to 23% of the total energy expenditure of the human body [36]. It requires a continuous fuel supply to meet its energy demands. In AD, reduced metabolism plays a major role in cellular and functional degeneration. The cerebral metabolic rate for glucose, the main substrate used to establish and maintain transmembrane ionic gradients [37], is notably low in AD hippocampus (27%–30%), as well as in the temporal, parietal, and posterior cingulate cortex [38]. As others have shown, we report expression differences for glycolytic and citric acid cycle enzymes in AD [365], which may underpin glucose hypometabolism.

Enolases and succinyl- coenzyme A:3-ketoacid-coenzyme A transferase 1 are involved in glucose metabolism. A whole-tissue proteome study reported greater expression of α- and γ-enolases and succinyl coenzyme A:3-ketoacid-coenzyme A transferase 1 in hippocampus and temporal cortex in AD [39]. Using subcellular fractionation, we find a significantly higher expression of α-enolase in AD temporal cortex, lower expression of γ-enolase in AD hippocampus, and lower expression of succinyl coenzyme A:3-ketoacid-coenzyme A transferase 1 in AD temporal cortex. The altered expression of pyruvate kinase isoform M1, the catalytic enzyme for the last step of glycolysis, has not been reported in previous studies. The expression of this protein was significantly lower in AD hippocampus and temporal cortex synapses. A previous whole-tissue proteome study reported lower expression of the glycolytic enzyme phosphoglycerate mutase 1 in AD hippocampus [8], whereas by focusing down at the synaptic level, we found higher expression of the same protein.

We detected quantitative differences in the expression of malate dehydrogenase, a citric acid cycle enzyme, in AD-affected regions of the human brain. Malate dehydrogenase is subject to lipid peroxidation in AD [40], which may affect its function further. In addition to expression differences, most glycolytic enzymes are oxidized in hippocampus and temporal cortex in AD. This would alter their function further and reduce glucose metabolism. These alterations indicate that glycolytic function is altered in affected regions of the AD brain. Within the synapse, even mildly impaired glucose metabolism can have a critical impact on the synthesis of acetylcholine, a memory-associated neurotransmitter [41]. Low glucose levels can promote hyperphosphorylation of tau proteins in vitro and in vivo [42].

Creatine kinase B, involved in energy transfer, showed a significant expression difference in AD. Creatine kinase B oxidation has been detected in AD brain [43]; however, this is the first report of reduced expression in AD hippocampus synapses. Lower creatine kinase B expression and post-translational modification could combine to alter cellular metabolism. Weakened energy metabolism could reduce ATP production and decreases the capacity of the synapse

to respond to energy requirements, thus compounding the effects of reduced glucose metabolism.

4.4. Antioxidants

In recent years there has been heightened interest in the functional importance of free radical-driven oxidative stress in AD pathogenesis. During energy production, cytotoxic free radicals leak constantly from mitochondria. A high number of mitochondria are present in nerve endings to meet the high energy demand required for synaptic activity [44]. Nerve endings are vulnerable to free radical-driven oxidative stress because of their abundant lipid content, high rate of oxygen consumption, and relative lack of antioxidants. Our observation of higher expression of peroxiredoxin 1 reflects the severity of free radical-induced oxidative stress in AD hippocampus, and the protective mechanisms deployed to combat it.

4.5. Signal transduction

Synaptic proteins involved in signal transduction, including rab GDP dissociation inhibitor β and ρ guanine nucleotide dissociation inhibitor 1, showed disease-specific expression differences. GDPs bind to inactive GDP-bound rab/ρ proteins and slow the rate of GDP dissociation. We found a higher level of rab guanine nucleotide dissociation inhibitor β expression in AD hippocampus and temporal cortex, which may reduce the amount of active rab protein available, reducing neuroprotection, attenuating long-term depression [45], and altering the endocytic pathway [46]. ρ Guanine nucleotide dissociation inhibitor 1 was identified in two spots with the same isoelectric point but different molecular weights (Fig. 3B). One spot showed no significant difference whereas the other showed lower expression in AD temporal cortex. This result suggests that enhanced positive neuritic outgrowth regulation in AD may result from lower expression of specific isoforms and/or posttranslationally modified ρ guanine nucleotide dissociation inhibitor protein [47] as a neuroprotective mechanism in response to synaptic degeneration.

4.6. Chaperones

The expression of ubiquitin regulatory X (UBX)-domain-containing protein 6 (UBXD6) was 22.4% higher in non-AD temporal cortex, but no change was detected in AD hippocampus (data not significant). UBXD6 is expressed abundantly in testis and ovary, suggesting a role in reproduction [48]. The presence of this protein in the synaptic fraction implies that it has other functions yet to be determined. The ubiquitinlike UBX domain suggests its involvement in ubiquitin-related processes, including endocytosis and protein degradation [49]. Higher expression of UBXD6 in AD reflects a possible compensatory mechanism for the failure of other ubiquitination enzymatic systems in AD. Despite the significant disease-related expression difference in AD synapses shown here, it has not been associated with AD in previous studies.

We report lower synaptic expression of the heat shock cognate 71 kDa protein in AD temporal cortex, whereas whole-tissue studies detected higher expression in the temporal lobe [50]. Heat shock proteins act as molecular chaperones, mediating correct protein folding and transferring misfolded proteins to the proteasome for degradation [51]. A lower level of heat shock cognate 71 kDa protein in AD temporal cortex may cause misfolded proteins to aggregate, and these might include Aβ and plaque formation, which are pathological hallmarks of AD.

4.7. Concluding remarks

A major advantage of 2D electrophoresis is that multiple protein expression forms, derived from posttranslational modification isoforms and/or alternate splicing, can often be visualized. Often, these proteins are found in trains of spots with the same molecular weight but different isoelectric points (Fig. 3). Of the proteins of interest, we identified several proteins on the 2D gel from more than one spot. Follow-up of these proteins and posttranslational modifications will be beneficial for understanding the mechanisms of cell regulation and synaptic degeneration in AD.

In summary, we used subcellular fractionation combined with comparative proteomics to study the synaptic proteome of human Alzheimer's disease brain obtained at autopsy. We documented quantitative expression differences in synaptic proteins from two severely affected brain regions. We identified 36 synaptic proteins exhibiting significant expression differences, some of which have been implicated in other studies and some that were novel proteins. The identification of synaptic proteins exhibiting disease-specific differences poses questions of how this might alter the function of the AD synapse. We conclude that the synaptic proteome from AD brain is significantly different from that in the normal aging brain, and that the proteins identified can be used for disease marker and drug-target development.

Acknowledgments

Financial support was provided by the Alzheimer's Association (USA) under grant no. RG1-96-005 and the Judith Jane Mason and Harold Stannett Williams Memorial Foundation. The Australian Brain Bank Network, of which the Queensland Brain Bank is a node, is supported by a National Health Medical Research Council (Australia) enabling grant (no. 605210).

References

[1] Fratiglionni L, De Ronchi D, Aguero-Torress H. Worldwide prevalence and incidence of dementia. Drugs Aging 1999;15:365–75.

[2] DeKosky ST, Scheff SW. Synapse loss in frontal cortex biopsies in Alzheimer's disease: correlation with cognitive severity. Ann Neurol 1990;27:457–64.

[3] Honer WG, Dickson DW, Gleeson J, Davies P. Regional synaptic pathology in Alzheimer's disease. Neurobiolog Aging 1992;13:375–82.
[4] Davis CA, Mann DM, Sumpter PA, Yates PO. A quantitative morphometric analysis of the neuronal and synaptic content of the frontal and temporal cortex in patients with Alzheimer's disease. J Neurol Sci 1987;78:151–64.
[5] Cook IA, Leuchter AF. Synaptic dysfunction in Alzheimer's disease: clinical assessment using quantitative EEG. Behav Brain Res 1996; 78:15–23.
[6] Yao PJ, Zhu M, Pyun EI, Brooks AI, Therianos S, Meyers VE, et al. Defects in expression of genes related to synaptic vesicle trafficking in frontal cortex of Alzheimer's disease. Neurobiol Dis 2003; 12:97–109.
[7] Shankar GM, Walsh DM. Alzheimer's disease: synaptic dysfunction and Ab. Mol Neurodegen 2009;4:48.
[8] Sultana R, Boyd-Kimball D, Cai J, Pierce WM, Klein JB, Merchant M, et al. Proteomics analysis of the Alzheimer's disease hippocampal proteome. J Alzheimers Dis 2007;11:153–64.
[9] Shiozaki A, Tsuji T, Kohno R, Kawamata J, Uemura K, Teraoka H, et al. Proteome analysis of brain proteins in Alzheimer's disease: subproteomics following sequentially extracted protein preparation. J Alzheimers Dis 2004;6:257–68.
[10] Huber LA, Pfaller K, Vietor I. Organelle proteomics: implications for subcellular fractionation in proteomics. Circ Res 2003;92:962–8.
[11] Prokai L, Zharikova AD, Stevens SMJ. Effects of chronic morphine exposure on the synaptic plasma-membrane subproteome of rats: a quantitative protein profiling study based on isotope-coded affinity tags and liquid chromatography/mass spectrometry. J Mass Spectr 2005;40:169–75.
[12] Boyd-Kimball D, Castegna A, Sultana R, Poon HF, Petroze R, Lynn BC, et al. Proteomic identification of proteins oxidized by Aβ(1–42) in synaptosomes: implications for Alzheimer's disease. Brain Res 2005;1044:206–15.
[13] Muller T, Jung K, Ullrich A, Schrotter A, Meyer HE, Stephan C, et al. Disease state, age, sex, and post-mortem time-dependent expression of proteins in AD vs. control frontal cortex brain samples. Current Alzheimer Res 2008;5:562–71.
[14] Sokolow S, Luu SH, Headley AJ, Hanson AY, Kim T, Miller CA, et al. High levels of synaptosomal Na^{+}-Ca^{2+} exchangers (NCX1, NCX2, NCX3) co-localized with amyloid-beta in human cerebral cortex affected by Alzheimer's disease. Cell Calcium 2011;49:208–16.
[15] Halliday G, Ng T, Rodriguez M, Harding A, Blumbergs P, Evans W, et al. Consensus neuropathological diagnosis of common dementia syndromes: testing and standardising the use of multiple diagnostic criteria. Acta Neuropathol 2002;104:72–8.
[16] Dodd PR, Hardy JA, Baig EB, Kidd AM, Bird ED, Watson WEJ, et al. Optimization of freezing, storage, and thawing conditions for the preparation of metabolically active synaptosomes from frozen rat and human brain. Neurochem Pathol 1986;4:177–98.
[17] Hynd MR, Lewohl JM, Scott HL, Dodd PR. Biochemical and molecular studies using human autopsy brain tissue. J Neurochem 2003; 85:543–62.
[18] Hardy JA, Dodd PR. Metabolic and functional studies on post-mortem human brain. Neurochem Int 1983;5:253–66.
[19] Etheridge N, Lewohl JM, Mayfield RD, Harris RA. Synaptic proteome changes in the superior frontal gyrus and occipital cortex of the alcoholic brain. Proteom Clin Appl 2009;3:730–42.
[20] Strohalm M, Kavan D, Novak P, Volny M, Havlicek V. mMass 3: a cross-platform software environment for precise analysis of mass spectrometric data. Anal Chem 2010;82:4648–51.
[21] Perkins DN, Pappin DJ, Creasy DM, Cottrell JS. Probability-based protein identification by searching sequence databases using mass spectrometry data. Electrophoresis 1999;20:3551–67.
[22] Tilleman K, Van den Haute C, Geerts H, van Leuven F, Esmans EL, Moens L. Proteomics analysis of the neurodegeneration in the brain of tau transgenic mice. Proteomics 2002;2:656–65.
[23] Martin B, Brenneman R, Becker KG, Gucek M, Cole RN, Maudsley S. iTRAQ analysis of complex proteome alterations in 3xTgAD Alzheimer's mice: understanding the interface between physiology and disease. PLOS One 2008;3:1–21.
[24] Masliah E, Mallory M, Alford M, DeTeresa R, Hansen LA, McKeel Jr. DW, et al. Altered expression of synaptic proteins occurs early during progression of Alzheimer's disease. Neurology 2001; 56:127–9.
[25] Yao PJ, Zhu M, Pyun EI, Brooks AI, Therianos S, Meyers VE, et al. Defects in expression of genes related to synaptic vesicle trafficking in frontal cortex of Alzheimer's disease. Neurobiol Dis 2003; 12:97–109.
[26] Yamagata SK, Parsons SM. Cholinergic synaptic vesicles contain a V-type and a P-type ATPase. J Neurochem 1989;53:1354–62.
[27] Michaelson DM, Angel I. Determination of δ pH in cholinergic synaptic vesicles: its effect on storage and release of acetylcholine. Life Sci 1980;27:39–44.
[28] Gotow T, Sakata M, Funakoshi T, Uchiyama Y. Preferential localization of annexin V to the axon terminal. Neuroscience 1996;75:507–21.
[29] Demange P, Voges D, Benz J, Liemann S, Gottig P, Berendes R, et al. Annexin V: the key to understanding ion selevtivity and voltage regulation? Trends Biochem Sci 1994;19:272–6.
[30] Bedrood S, Jayasinghe S, Sieburth D, Chen M, Erbel S, Butler PC, et al. Annexin A5 directly interacts with amyloidogenic proteins and reduces their toxicity. Biochemistry 2009;48:10568–76.
[31] Ito H, Atsuzawa K, Morishita R, Usuda N, Sudo K, Iwamoto I, et al. Sept8 controls the binding of vesicle-associated membrane protein 2 to synaptophysin. J Neurochem 2009;108:867–80.
[32] Hempen B, Brion JP. Reduction of acetylated alpha-tubulin immunoreactivity in neurofibrillary tangle-bearing neurons in Alzheimer's disease. J Neuropathol Exp Neurol 1996;55:964–72.
[33] Butler D, Bendiske J, Michaelis ML, Karanian DA, Bahr BA. Microtubule-stabilizing agent prevents protein accumulation-induced loss of synaptic markers. Eur J Pharmacol 2007;562:20–7.
[34] Li X, Serwanski DR, Miralles CP, Nagata K, De Blas AK. Septin 11 is present in GABAergic synapses and plays a functional role in the cytoarchitecture of neurons and GABAergic synaptic connectivity. J Biol Chem 2009;284:17253–65.
[35] Su KY, Chien WL, Fu WM, Yu IS, Huang HP, Huang PH, et al. Mice deficient in collapsin response mediator protein-1 exhibit impaired long-term potentiation and impaired spatial learning and memory. J Neurosci 2007;27:2513–24.
[36] Sokoloff L. Energetics of functional activation in neural tissues. Neurochem Res 1999;24:321–9.
[37] Shulman RG, Rothman DL, Behar KL, Hyder F. Energetics of brain activity implications for neuroimaging. Trends Neurosci 2004; 27:489–95.
[38] Li R, Rinne JO, Mosconi L, Pirraglia E, Rusinek H, DeSanti S, et al. Regional analysis of FDG and PIB-PET images in notmal aging, mild cognitive impairment, and Alzheimer's disease. Eur J Nucl Med Mol Imaging 2008;35:2169–81.
[39] Schonberger SJ, Edgar PF, Faull RLM, Cooper GJS. Proteomic analysis of the brain in Alzheimer's disease: molecular phenotype of a complex disease process. Proteomics 2001;1:1519–28.
[40] Reed TT, Pierce WM, Markesbery WR, Butterfield DA. Proteomic identification of HNE-bound proteins in early Alzheimer disease: insights into the role of lipid peroxidation in the progression of AD. Brain Res 2009;1274:66–76.
[41] Sims NR, Bowen DM, Davison AN. [14C]Acetylcholine synthesis and [14C]carbon dioxide production from [U-14C]glucose by tissue prisms from human neocortex. Biochem J 1981;196:867–76.
[42] Liu F, Iqbal K, Grundke-Iqbal I, Hart GW, Gong CX. O-GlcNAcylation regulates phosphorylation of tau: a mechemism involved in Alzheimer's disease. Proc Natl Acad Sci USA 2004;101:10804–9.
[43] Castegna A, Aksenov M, Aksenova M, Thongboonkerd V, Klein JB, Pierce WM, et al. Proteomic identification of oxidatively modified proteins in Alzheimer's disease brain. Part I: creatine kinase BB, glutamine synthase, and ubiquitin carboxyl-terminal hydrolase L-1. Free Rad Biol Med 2002;33:562–71.

[44] Coyle JT, Puttfarcken P. Oxidative stress, glutamte, and neurodegenerative disorders. Science 1993;262:689–95.
[45] Baskys A, Bayazitov I, Zhu E, Fang L, Wang R. Rab-mediated endocytosis: linking neurodegeneration, neuroprotection, and synaptic pasticity. Ann N Y Acad Sci 2007;1122:313–29.
[46] Kimura N, Inoue M, Okabayashi S, Ono F, Negishi T. Dynein dysfunction induces endocytic pathology accompanied by an increase in rab GTPases: a potential mechanism underlying age-dependent endocytic dysfunction. J Biol Chem 2009;284:31291–302.
[47] Woo S, Gomez TM. Rac1 and RhoA promote neuritic outgrowth through formation and stabilization of growth cone point contacts. J Neurosci 2006;26:1418–28.
[48] Yamabe Y, Ichikawa K, Sugawara K, Imamura O, Shimamoto A, Suzuki N, et al. Cloning and characterization of Rep-8 (D8S2298E) in the human chromosome 8p11.2-p12. Genomics 1997;39:198–204.
[49] Hofmann K, Bucher P. The UBA domain: a sequence motif present in multiple enzyme classes of the ubiquitination pathway. Trends Biochem Sci 1996;21:172–3.
[50] Perez N, Sugar J, Charya S, Johnson G, Merril C, Bierer L, et al. Increased synthesis and accumulation of heat shock 70 proteins in Alzheimer's disease. Mol Brain Res 1991;11:249–54.
[51] Becker J, Craig EA. Heat-shock proteins as molecular chaperones. Eur J Biochem 1994;219:11–23.